PHYSICAL REVIEW B **88**, 081302(R) (2013)

Photoluminescence enhancement of silicon nanocrystals placed in the near field of a silicon nanowire

Houssem Kallel,[1,2,3] Arnaud Arbouet,[1,2] Marzia Carrada,[2] Gérard Ben Assayag,[2] Abdallah Chehaidar,[3] Priyanka Periwal,[4] Thierry Baron,[4] Pascal Normand,[5] and Vincent Paillard[1,2,*]

[1]*Université de Toulouse, Université Paul Sabatier, 118 route de Narbonne, 31062 Toulouse cedex 9, France*

[2]*CEMES-CNRS, 29 rue Jeanne Marvig, 31055 Toulouse Cedex 4, France*

[3]*Faculté des Sciences de Sfax, Université de Sfax, BP 1171, 3000 Sfax, Tunisia*

[4]*LTM/CNRS-CEA-LETI, 17 rue des martyrs, 38054 Grenoble, France*

[5]*National Center for Scientific Research "Demokritos", Department of Microelectronics, P.O. Box 60228, 15310 Aghia Paraskevi, Greece*

(Received 18 February 2013; revised manuscript received 10 June 2013; published 13 August 2013)

Semiconductor nanowires have an excellent ability to trap, guide, scatter, or absorb light for specific morphology-dependent resonant optical modes. The electromagnetic field enhancement associated with these modes could be used to modify the luminescence of emitters positioned in the vicinity of the nanowire, in a way similar to plasmonic nanostructures. We show that the photoluminescence of a single plane of silicon nanocrystals in silica, positioned at about 3 nm below the surface, can be enhanced by a factor of 2 to 3 in the presence of a silicon nanowire antenna on the silica surface. This could be the basis of a promising fully complementary metal oxide semiconductor compatible process to improve silicon-based light emitting devices, despite a lower enhancement compared to plasmonic nanostructures. Two-dimensional photoluminescence maps recorded for different polarization configurations (incident electric field parallel or perpendicular to the nanowire axis) exhibit different behaviors and can be related to the electric field intensity distribution in the near-field region of the nanowire, where the active silicon nanocrystal layer is located.

DOI: 10.1103/PhysRevB.88.081302 PACS number(s): 78.55.Ap, 78.67.Uh, 78.67.Bf, 78.35.+c

Semiconductor nanowires, in particular silicon nanowires, have attracted much attention in the last decade for their electronic properties and their potential application in nanoelectronics for gate-all-around transistors.[1] On the other hand, significant recent works have been devoted to their original optical properties for applications in photodetection,[2,3] solar cells,[4] or field-enhanced spectroscopy.[5,6] Indeed, Si,[7] Ge,[2] $Si_{1-x}Ge_x$,[8] or GaAs[9] nanowires of diameters ranging from a few tens to a few hundreds of nanometers can efficiently trap visible and infrared light thanks to their high refractive index in the range of 3.5 to 5. In addition, the very low extinction coefficient in the same wavelength range makes them highly suitable for low-loss nanometer-scale optical resonators or antennas.

The leaky mode resonances (LMRs) have been calculated using either the analytical Lorenz-Mie theory[2,7,8] or numerical simulations such as the finite-difference time-domain (FDTD) method.[10,11] Both theoretical and numerical simulation approaches allow one to draw complex 2D maps giving the scattering and absorption efficiencies as functions of nanowire diameter and wavelength. Most of the works have been devoted to photovoltaic applications to show a correlation between enhanced optical absorption and enhanced photocurrent inside a nanowire.[2,10] Similarly, the enhanced Raman scattering efficiencies of Si nanowires was due to the enhanced internal electromagnetic field.[11,12]

On the other hand, Si nanowires can be used as dielectric antennas. In that case, the external field enhancement in the vicinity of the nanowire can be used to enhance the Raman signal of molecules or molecule-capped nanoparticles decorating the nanowire,[5] or to locally enhance the photocurrent in the Si layer of a silicon-on-insulator substrate.[3] Field-enhanced spectroscopy was also performed in the case of vertical silicon nanopillars using the fundamental guided mode instead of the LMRs. Wells *et al.* showed that Raman or fluorescence spectra could be significantly enhanced, with an enhancement comparable to what could be obtained using common plasmonic nanostructures.[6] Surprisingly, it seems that semiconductor nanowire (NW) antennas have rarely been used to increase the luminescence of an emitter, whether a molecule or quantum dot. We show in the following that Si-NWs can be used for that purpose, and we apply it to the photoluminescence enhancement of silicon nanocrystals.

Silicon nanocrystals (Si-NCs) are still the subject of intense research in order to use them in Si-based light emitting diodes,[13,14] in photovoltaic devices for enhanced absorption[15] and down-conversion of solar radiation,[16] or as biomedical tagging applications.[17] Despite high quantum yield obtained for some plasma-synthesized Si-NCs,[18] the intensity of the light emitted by silica-embedded Si-NCs has to be increased. This could be achieved by improving the emission rate thanks to a modification of the local electromagnetic environment of the Si-NCs. Recent attempts using various plasmonic antennas placed above the Si-NCs showed that the photoluminescence (PL) was multiplied by a factor of 2 to 8 depending on the incident power density and the distance between the plasmonic nanostructures and the Si nanocrystals.[14,19] Compared to plasmonic nanostructures made of noble metals, Si-NWs should be interesting for several reasons: complementary metal oxide superconductor process compatibility, possible fabrication directly from the Si substrate, larger probing volume, and low losses due to the lower absorption of the emitted light by the antenna.

A single plane of Si-NCs embedded in silica is formed by ultralow-energy implantation of Si ions in a 10 nm thick SiO_2 layer thermally grown on a Si substrate, followed by thermal annealing.[20,21] It is located at about 3 nm below the silica surface and the Si-NCs have a mean diameter of about 2.3 nm. Transmission electron microscope (TEM) images showing the Si-NC plane are presented in Fig. 1. The surface concentration of about 1.9 10^{12} cm^{-2} as well as the distance between the

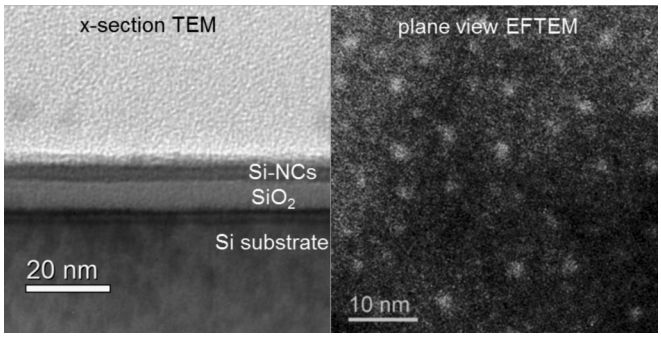

FIG. 1. Cross section and plane view energy-filtered transmission electron microscope images of the Si-NC plane formed by Si ion implantation (5×10^{15} cm^{-2}, 1 keV) in SiO_2 followed thermal annealing in N_2 at 1050 °C for 90 min.

NCs and the surface are constant. Such system exhibits an intense PL centered around 725 nm (1.72 eV) and a typical PL spectrum is shown in Fig. 2(b).

The Si-NWs are grown in a hot-wall reduced pressure chemical vapor deposition (RP-CVD) system via the vapor-liquid-solid process. After deposition of (i) a 2 nm thick Au layer or (ii) Au colloids calibrated in diameter, the Si (111) substrate was loaded in the deposition chamber and annealed to form the gold catalysts. Following the droplet formation step, the system was cooled down to the deposition temperature. The samples were then exposed to the reactive gases (SiH_4 and H_2 used as a carrier gas) to grow NWs of the desired diameter.[22] Nanowires of 100 nm mean diameter were grown for the purpose of this work. The gold nanoparticles at the

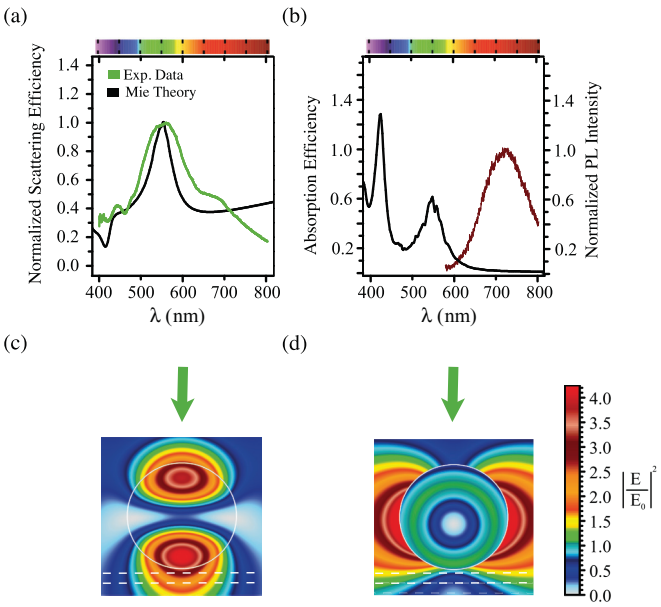

FIG. 2. (Color online) (a) Experimental scattering spectrum (green curve) compared to the theoretical spectrum of a 100 nm diameter Si-NW in air. (b) Calculated absorption spectrum (black curve) of a 100 nm diameter Si-NW in air superimposed on the PL spectrum of the Si-NC sample (red curve). Normalized electric field intensity distribution in the NW cross section at 532 nm for the TM_{11} mode (c) and for the TE_{01} mode (d). The dashed horizontal lines delimit the Si-NC plane.

nanowire extremities are always removed before the step of the nanowire solution formation by dilution and sonication in isopropanol.

Isolated nanowires are drop coated on the substrate containing the Si-NC plane. The diameter of a NW is measured by comparing its experimental elastic light scattering spectrum to the theoretical scattering efficiency calculated using Mie theory. As in other works,[2,7] a very good agreement between experiment and theory is obtained considering Si-NWs in air, although the NWs are herein deposited on a silica substrate containing the Si-NC plane close to the Si substrate. The optical spectroscopy experiments are performed on a customized Horiba-Jobin Yvon Xplora MV2000 allowing alternatively photoluminescence spectrometry and light scattering spectroscopy by switching from bright-field to dark-field illumination. Photoluminescence spectra are obtained using a 532 nm excitation focused through a 100×, 0.9 numerical aperture (NA), bright-field (BF) objective, and a power on the sample limited to few hundred nanowatts in order to prevent any PL quenching or blinking effect. The dark-field (DF) scattering spectra are obtained with a 50×, 0.6 NA, DF objective and a halogen lamp. Confocal microscopy is used in both BF/DF configurations, which also share a 300 groves/mm grating. More details about both the spectrometer and light scattering experiments can be found in previous works.[8] In the following, we focus on Si-NWs of about 100 nm diameter, since their scattering spectrum exhibits a resonance near 532 nm corresponding to the laser excitation wavelength for PL experiments [see Fig. 2(a)]. This resonance corresponds to a degenerated TM_{11}-TE_{01} mode.[7,8] Furthermore, the Si-NW absorption is negligible in the PL wavelength range [see Fig. 2(b)], thus preventing any emitted light reabsorption.

Photoluminescence maps such as presented in Fig. 3 are obtained by scanning the sample using a step of 100 nm and recording a spectrum at each point. The color scale corresponds to the integrated intensity of the PL band centered at 725 nm. First of all, it should be noticed that the PL background far from the nanowire is constant. It is a proof, in addition to the TEM images, that Si-NCs are homogeneously distributed in the sample. Second, it should be mentioned that no PL can be detected from any Si-NW deposited on a standard Si substrate, in absence of Si-NCs. It is obvious that depending on the polarization of the incident light, either perpendicular [TE, Fig. 3(a)] or parallel [TM, Fig. 3(b)] to the NW axis, it is evident that the Si-NC PL intensity is strongly affected by the presence of the nanowire. In the TE configuration, the TE_{01} mode is excited while it is the TM_{11} mode in the TM configuration.

The PL intensity, proportional to the emission rate Γ_{PL}, involves two factors:[19,23]

$$\Gamma_{PL} = \Gamma_{exc}(\Gamma_{rad}/\Gamma), \quad (1)$$

where Γ_{exc} is the excitation rate, Γ_{rad} the radiative decay rate, and $\Gamma = \Gamma_{rad} + \Gamma_{nonrad}$ the total decay rate, Γ_{nonrad} being the nonradiative decay rate.

The first term Γ_{exc} is function of the local excitation field. The other contribution to the PL enhancement could be attributed to the increase of the radiative decay rate Γ_{rad}, hence to a higher photon density of states.[19,23] As evidenced in Figs. 2(c) and 2(d), although Mie calculations are performed for a nanowire in air and do not reflect perfectly the geometry

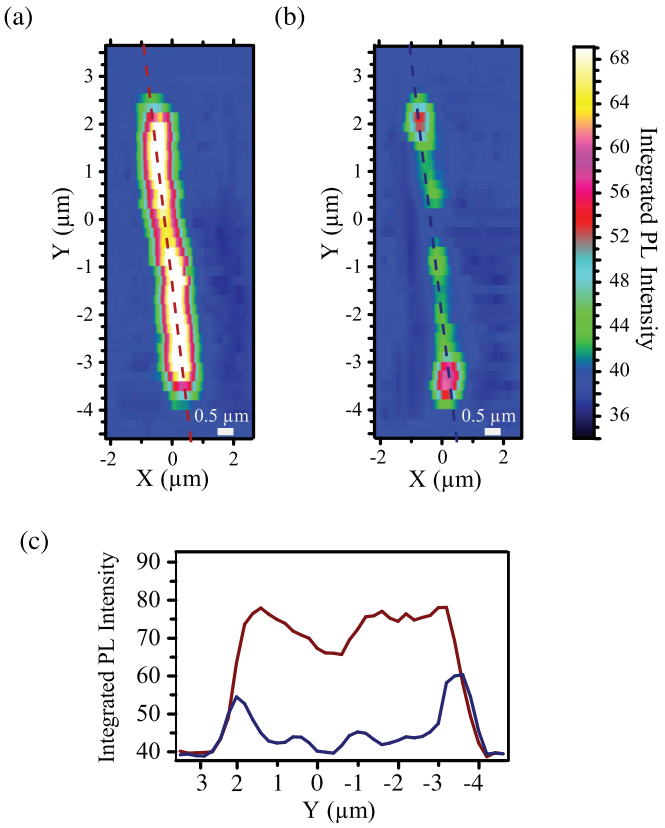

FIG. 3. (Color online) Photoluminescence maps of a Si-NC plane positioned 3 nm below a 100 nm diameter and 6 μm length Si nanowire for two polarization configurations. (a) TE configuration. (b) TM configuration. (c) Profile of the integrated PL intensity along the NW axis.

of our sample, the excitation laser field scattered by the NW is strongly confined in the near-field region of the nanowire, where is also the position of the Si-NC plane. There is an interesting correlation between the electric field intensity distribution and the PL maps. In particular the FWHM of the integrated PL intensity is obviously larger in the TE case, in agreement with the lateral extension of the electric field intensity of the TE_{01} mode. Moreover, since the enhanced emission could be attributed to a better extraction of light in the presence of the Si-NW at the surface, counterbalancing the Si substrate effect in the lower half space,[24,25] we performed additional experiments to prove that the PL enhancement is due to Γ_{exc}. An additional 20 nm thick SiO_2 layer was grown by TEOS deposition on top of the SiO_2-embedded Si-NC layer before drop coating of the nanowire solution. Hence we could compare the PL maps in presence of a NW deposited from the same solution and located at about 3 and 23 nm above the Si-NC plane, depending on the deposition or not of the 20 nm thick SiO_2 layer. The PL intensity profiles as function of the SiO_2 thickness t for two similar nanowires are shown in Fig. 4. The PL far from the NWs is the same in both samples, proving that the NC emission was not affected by the additional SiO_2 deposition. Considering the TE case, the integrated PL intensity is strongly decreased with increasing NW-NC plane distance t and could be correlated to the strong decrease of the electric field intensity with increasing depth according to Fig. 2(d).

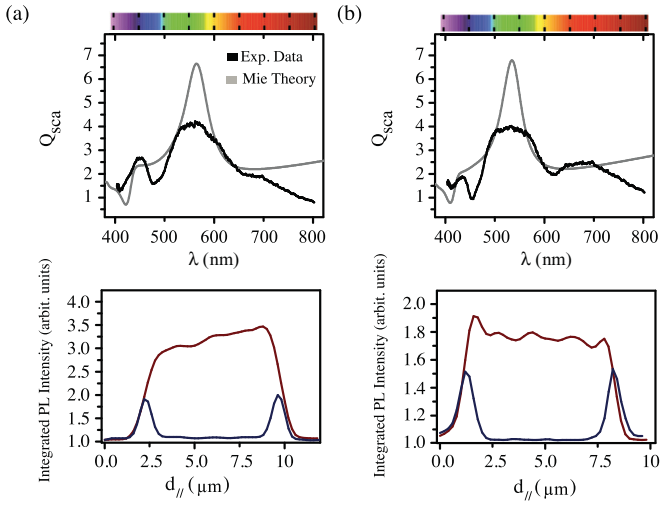

FIG. 4. (Color online) (a) describes a 103 nm diameter and 7.5 μm length NW separated from the NC plane by a 3 nm thick SiO_2 layer. (b) describes a 95 nm diameter and 7 μm length NW separated from the NC plane by a 23 nm thick SiO_2 layer (see text for details). Upper graphs: Scattering efficiencies. Lower graphs: Integrated PL intensity profiles along the NW axis (red curves: TE configuration, blue curves: TM configuration). The PL is normalized to the PL background far from the NWs, which is the same for both samples.

However, these remarks are not sufficient to fully explain the strong dependence on the incident laser polarization, nor the NW edge effects due do its finite length. As seen in Fig. 3, the PL intensity of the Si-NCs is homogeneously enhanced by the NW in the TE configuration, while the strong enhancement is limited to the Si-NCs located under the NW edges in the TM configuration. We show in the following that the difference in the PL profiles are very similar to the measured[27] or calculated[28,29] confined electric fields in the near-field region of dielectric nanostructures. In these works, it is shown that the normalized electric field intensity is maximum when the incident electric field is normal to any nanostructure surface separating two different media. This can be explained by the continuity condition of the normal component of the displacement vector $D_n = \epsilon E_n$ at the boundary between the nanostructure (medium 1) and the external medium (medium 2):

$$\epsilon_1 E_{n1} = \epsilon_2 E_{n2}. \quad (2)$$

If the nanostructure has a much higher dielectric constant than the surrounding medium, the external field near the nanostructure surface will be strongly enhanced. In our case, the PL intensity in the so-called TM configuration presented in Figs. 3(b), 3(c), and 4 shows a large enhancement at the nanowire edges and a weak or no enhancement along the wire between both edges. In this configuration, the incident laser polarization is parallel to the nanowire axis; hence the continuity of the tangential component of the electric field is always satisfied except at the nanowire edges where the electric field is purely normal. Therefore, the above equation applies and the electric field seen by the Si-NCs around the NW edges should be enhanced at the interface by roughly a factor of 3, according to the dielectric permittivity of 12 for Si and 4 for SiO_2.[26] Contrarily, the PL intensity in the

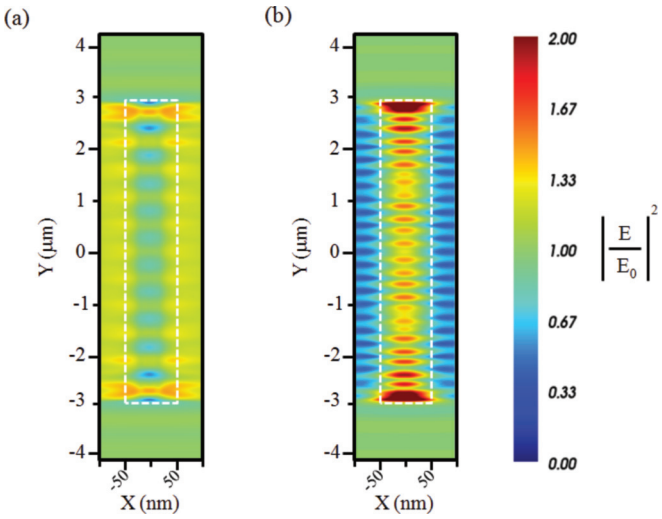

FIG. 5. (Color online) Normalized electric field intensity at 5 nm below a 6 μm long and 100 nm diameter Si nanowire for TE (a) and TM (b) polarizations of the incident light (532 nm wavelength). The NW projection is shown as dashed white line.

TE configuration [Figs. 3(a), 3(c), and 4] is homogeneous along the nanowire. In that case, the incident electric field is perpendicular to the nanowire axis so that the continuity of the normal component of the displacement vector is satisfied all along the nanowire. Hence, the field enhancement seen by the Si-NCs is homogeneous under the nanowire.

We used DDSCAT free software to model a 6 μm long and 100 nm diameter Si nanowire in vacuum, comparable to the NW studied in Fig. 3.[30,31] For such structure, the scattering and absorption efficiencies obtained using DDSCAT and Mie theory are in very good agreement over the 400–800 nm wavelength range, except for a slightly different value of the absorption efficiency for the TM_{01} mode. We thus mapped the normalized electric field intensity at 5 nm below the NW, as shown in Fig. 5. It is striking that for both TE and TM cases, the intensity distribution is very similar to the PL intensity map.

The field intensity distributions exhibit maxima at the NW edges, as for PL maxima. The calculated interference pattern cannot be detected by far-field experiments. However, some minima can be evidenced at about -1.5, 0, and 1.5 μm. Such a spacing roughly corresponds to the PL oscillations observed in both PL map and profile shown in Figs. 3(b) and 3(c), respectively. In the TE case, the electric field intensity is more homogenous with a slight decrease near the middle of the NW compared to its edges. This is also very similar to PL measurements presented in Figs. 3(a) and 3(c). These results prove that the local total field strongly influences the NC emission, although it should be kept in mind that the NW is illuminated by a plane wave in the numerical simulations, which is not the case of PL experiments involving a tightly focused laser beam.

In this Rapid Communication, we showed that the photoluminescence of Si nanocrystals positioned in the near field of a Si nanowire antenna can be increased by a factor of up to 3. We used an ideal system for this demonstration with a single plane of Si-NCs located in the vicinity of the Si-NW. This is a promising result that could be extended to thicker layers or multilayers of Si-NCs for improved silicon-based light emitting devices. Further works are planned by changing the position of the Si-NCs (for instance on each side of the NW where they could benefit of the high local electric field in the TE configuration), or coupling parallel NWs to increase the resonances. Finally, semiconductor NWs could be used with more efficient luminescent nanoparticles or molecules than Si-NCs, providing an interesting alternative to plasmonic nanostructures in different application domains.

H.K. and V.P. acknowledge financial support from French Ministry of Foreign Office, French Embassy in Tunis, and Université Paul Sabatier. DDSCAT calculations were performed using the CALMIP computing facilities under Grant No. P12167. We thank Dr. Christian Girard (CEMES-CNRS) for fruitful scientific discussions and comments.

*Corresponding author: vincent.paillard@cemes.fr

[1] J. Golberger, A. I. Hochbaum, R. Fang, and P. Yang, Nano Lett. **6**, 973 (2006).

[2] L. Cao, J.-S. White, J.-S. Park, J. A. Schuller, B. M. Clemens, and M. L. Brongersma, Nat. Mater. **8**, 643 (2009).

[3] E. S. Barnard, R. A. Pala, and M. L. Brogersma, Nat. Nanotechnol. **6**, 588 (2011).

[4] B. Tian, X. Zheng, T. J. Kempa, Y. Fang, N. Yu, G. Yu, J. Huang, and C. M. Lieber, Nature (London) **449**, 885 (2007).

[5] L. Cao, B. Garipcan, E. M. Gallo, S. S. Nonnenmann, B. Nabet, and J. E. Spanier, Nano Lett. **8**, 601 (2008).

[6] S. M. Wells, I. A. Merkulov, I. A. Kravchenko, N. V. Lavrik, and M. J. Sepaniak, ACS Nano **6**, 2948 (2012).

[7] G. Brönstrup, N. Jahr, C. Leiterer, A. Csáki, W. Fritzsche, and S. Christiansen, ACS Nano **8**, 601 (2010).

[8] H. Kallel, A. Arbouet, G. Ben Assayag, A. Chehaidar, A. Potié, B. Salem, T. Baron, and V. Paillard, Phys. Rev. B **86**, 085318 (2012).

[9] G. Brönstrup, C. Leiterer, N. Jahr, C. Gutsche, A. Lysov, I. Regolin, W. Prost, F. J. Tegude, W. Fritzsche, and S. Christiansen, Nanotechnol. **22**, 385201 (2011).

[10] T. J. Kempa, J. F. Kahoon, S.-K. Kim, R. W. Day, H.-G. Park, and C. M. Lieber, Proc. Natl. Acad. Sci. USA **109**, 1407 (2012).

[11] F. J. Lopez, J. K. Hyun, In Soo Kim, A. L. Holsteen, and L. J. Lauhon, Nano Lett. **12**, 2266 (2012).

[12] L. Cao, B. Nabet, and J. E. Spanier, Phys. Rev. Lett. **96**, 157402 (2006).

[13] M. Perálvarez, C. Garcia, M. López, B. Garrido, J. Barreto, C. Domínguez, and J. A. Rodríguez, Appl. Phys. Lett. **89**, 051112 (2006).

[14] C. Huh, C.-J. Choi, W. Kim, B. K. Kim, and B.-J. Park, Appl. Phys. Lett. **100**, 181108 (2012).

[15] F. Gourbilleau, C. Ternon, D. Maestre, O. Palais, and C. Dufour, J. Appl. Phys. **106**, 013501 (2009).

[16]T. Trupke, M. A. Green, and P. Würfel, J. Appl. Phys. **92**, 1668 (2002).
[17]F. Erogbogbo, K.-T. Yong, I. Roy, G. Xu, P. N. Prasad, and M. T. Swihart, ACS Nano **2**, 873 (2008).
[18]J. B. Miller, A. R. Van Sickle, R. J. Anthony, D. M. Kroll, U. R. Kortshagen, and E. K. Hobbie, ACS Nano **6**, 7389 (2012).
[19]J. S. Biteen, D. Pacefici, N. S. Lewis, and H. A. Atwater, Nano Lett. **5**, 1768 (2005).
[20]C. Bonafos, H. Coffin, S. Schamm, N. Cherkashin, G. Benassayag, P. Dimitrakis, P. Normand, M. Carrada, V. Paillard, and A. Claverie, Solid State Electron. **49**, 1734 (2005).
[21]M. Carrada, A. Wellner, V. Paillard, C. Bonafos, H. Coffin, and A. Claverie, Appl. Phys. Lett. **87**, 251911 (2005).
[22]F. Dhalluin, T. Baron, P. Ferret, B. Salem, P. Gentile, and J.-C. Harmand, Appl. Phys. Lett. **96**, 133109 (2010).
[23]P. Anger, P. Bharadwaj, and L. Novotny, Phys. Rev. Lett. **96**, 113002 (2006).
[24]E. Yablonovitch, T. J. Gmitter, and R. Bhat, Phys. Rev. Lett. **61**, 2546 (1988).
[25]I. Sychugov, A. Galeckas, N. Elfström, A. R. Wilkinson, R. G. Elliman, and J. Linnros, Appl. Phys. Lett. **89**, 111124 (2006).
[26]J. Humlícek, in *Properties of Silicon Germanium and SiGe:Carbon*, EMIS Datareviews Series, edited by E. Kasper and K. Lyutovich, No. 24 (INSPEC, London, 2000), pp. 244–259.
[27]J.-C. Weeber, E. Bourillot, A. Dereux, J.-P. Goudonnet, Y. Chen, and C. Girard, Phys. Rev. Lett. **77**, 5332 (1996).
[28]O. J. F. Martin, C. Girard, and A. Dereux, J. Opt. Soc. Am. A **13**, 1801 (1996).
[29]C. Girard, A. Dereux, O. J. F. Martin, and M. Devel, Phys. Rev. B **52**, 2889 (1995).
[30]B. T. Draine and P. J. Flatau, J. Opt. Soc. Am. A **11**, 1491 (1994).
[31]P. J. Flatau and B. T. Draine, Opt. Express **12**, 1247 (2012).